J. Fluid Mech. (1964), *vol.* 20, *part* 2, *pp.* 281–289
Printed in great Britain

Modes of instability in spiral flow between rotating cylinders

By K. W. SCHWARZ, B. E. SPRINGETT AND R. J. DONNELLY

Institute for the Study of Metals and Department of Physics, University of Chicago

(Received 6 March 1964)

A study of the stability of flow between concentric cylinders, with the inner one rotating, distinguished three kinds of instabilities: the famililar axisymmetric mode, an azimuthal mode with the predicted $\exp i(\theta - \omega t)$ angular dependence, and a completely non-symmetric instability which apparently arises from the interaction of the other two. The effect of small axial flow upon all of these modes was to give an approximately parabolic dependence of the critical Taylor number on the axial flow rate. In the case of the axisymmetric mode, agreement with the theory of Krueger & Di Prima (1964) was found to be excellent.

1. Introduction

This paper gives the results of an experimental investigation of the stability of spiral flow between rotating cylinders with respect to axisymmetric and non-axisymmetric disturbances. Various modes of instability were detected by observing visually characteristic ink patterns in the fluid. The usual parameters characterizing the motion of the fluid are the Taylor number

$$T = \frac{2\eta^2 d^4}{1-\eta^2}\left(\frac{\Omega}{\nu}\right)^2 \tag{1}$$

and the axial Reynolds number

$$R_x = V_m d/\nu, \tag{2}$$

where η is the ratio of the radii R_1 and R_2 of the inner and outer cylinders; $d = (R_2 - R_1)$; Ω is the angular velocity of the inner cylinder, the outer one being kept stationary; ν is the kinematic viscosity; and V_m is the mean axial velocity. The critical Taylor number T_c at which a given mode first becomes self-sustaining depends on R_x and on the type of instability the mode represents. We have studied the behaviour of the types of instability found experimentally, determining quantitatively the dependence of T_c on R_x over a limited range of $R_x (0 \leqslant R_x < 25)$.

The stability with respect to axisymmetric disturbances has been investigated experimentally by Donnelly & Fultz (1960*a*, *b*) and by Snyder (1962), and theoretically by Chandrasekhar (1960, 1962), by DiPrima (1960), and by Krueger & DiPrima (1964). Non-axisymmetric modes of instability have been discussed by DiPrima (1961) and by Donnelly & Schwarz (1964) for the case of zero axial

flow, but the effect of axial flow on these modes has not been calculated. In our experiment $\eta \sim 0{\cdot}95$, so that the theories based on the narrow-gap approximation are applicable.

2. Apparatus

The apparatus, shown schematically in figure 1, is nearly identical to that described in detail by Donnelly & Fultz (1960*b*) and more recently by Snyder (1962). The only significant modification was the introduction of calibrated copper-constantan thermocouples H and G near the top and bottom of the cylinders to allow accurate temperature measurements. The height of the concentric cylinder system is about 90 cm. The outer cylinder is made of Pyrex and has an inside radius of $6{\cdot}3137 \pm 0{\cdot}0004$ cm. This cylinder was made by purchasing a precision-bore glass cylinder from the Fischer–Porter Company, honing the inside with a cast-iron hone especially constructed to produce a straight bore, and then pitch-polishing the inner surface with a modified Sunnen hone. Two inner cylinders were used, one of chromium-coated aluminium with a radius of $5{\cdot}9682 \pm 0{\cdot}0006$ cm, and one of stainless steel with a radius of $5{\cdot}9684 \pm 0{\cdot}0006$ cm. They yielded identical results, and hence we have not indicated on our curves which cylinder was used for a given determination. The values of R_1 and R_2 quoted above were obtained by making measurements at 144 equally spaced points on the cylinders.

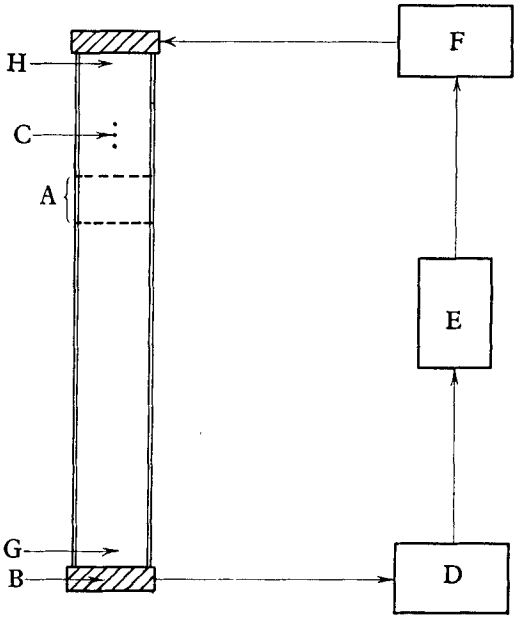

FIGURE 1. Schematic diagram of the apparatus: A, observation region; B, bottom bearing; C, ink ports; D, pump; E, constant temperature bath; F, flow meter and thermometer; G, lower thermocouple; H, upper thermocouple.

To minimize systematic errors in d, we restricted our observations to a region lying 62·0–68·5 cm above the bottom of the cylinders. In this region, labelled A

in figure 1, volumetric measurements were made to determine the correct average values of d. The values obtained were $d = 0{\cdot}3462 \pm 0{\cdot}0005$ cm for the aluminium cylinder, and $d = 0{\cdot}3463 \pm 0{\cdot}0005$ cm for the stainless-steel cylinder, in satisfactory agreement with the values predicted on the basis of R_1 and R_2 as given above. The position of our observation region had the advantages of being a reasonable distance from the point C where the tracer ink was injected, and of being far removed from the only significant heat source, the bearing B at the bottom of the cylinder.

3. Experimental procedures

3.1. *Temperature determination*

Formulas (1) and (2) depend on temperature through the kinematic viscosity, which changes by about 2·5 % per °C for distilled water. Hence, it is crucial that the temperature t_A in the region of observation be accurately determined. Heat is produced mainly by the bearing at the bottom of the cylinders and is removed downstream by the constant temperature bath. The fluid can also exchange heat with the atmosphere via the containing walls, although this effect was minimized by keeping the fluid temperature near that of the surrounding air. An external vertical temperature gradient was avoided by using fans to supplement the air-conditioning of the laboratory. The fluid temperature was monitored at frequent intervals in three places: t_F at the flow-meter F, t_H at the top of the cylinders H, and t_G at the bottom of the cylinders G.

For $R_x \geqslant 7$, we required that t_F and t_H agree to within 0·05 °C. Since the fluid had ample opportunity for coming to equilibrium with its surroundings by the time that it had reached H, and since there were no other sources or sinks of heat between H and the region of observation, we concluded that $t_A = t_H$ to better than 0·05 °C.

For $R_x \leqslant 7$, the fluid is moving so slowly that it becomes difficult to keep t_F and t_H within 0·05 °C. Instead, we circulated the fluid briskly until t_A and t_H were very close. Reducing the flow-rate to the desired value, we monitored t_H continuously. If it drifted less than 0·07 °C during the entire run (typical duration $\sim$ 20 min), we assumed $t_A = t_H$, since both points are subject to the same sort of heat exchange with the atmosphere. If the drift was greater, the results were discarded. In the region $R_x \sim 7$ where these two methods overlapped, they gave equivalent results. With these precautions, the authors estimate that the temperature in the region of observation was known to better than $\pm$ 0·05 °C.

3.2. *Determination of* Ω_c

(i) *Axisymmetric mode.* The critical angular velocity of a given mode was assumed to be the value of Ω at which its characteristic ink pattern was first observed. The procedure was to advance Ω by steps of $\sim \frac{1}{2}$ % near the expected critical point, waiting at least 5 min after each change. The critical value of Ω was then taken to lie between the value at which the cell pattern was first observed and the next lower value. Several factors complicated this procedure: (*a*) the amplitude of the circulation in the cell approaches zero at the critical point;

(*b*) the cell growth is very slow near critical, and during the long development natural diffusion of the tracer ink may obscure the pattern; (*c*) the abrupt injection of large amounts of ink gives rise to transient patterns; (*d*) at very low flow-rates, small irregularities on the walls (e.g. the ink ports) give rise to local cell patterns which slowly propagate up and down the cylinders. For the narrow-gap case, the amplitude and growth-rate of the cells increase rapidly beyond the critical point (see Donnelly & Schwarz 1964), so that factors (*a*) and (*b*) introduced negligible systematic error. At high flow-rates, the problem posed by transient cells was minimized by slowly feeding into the fluid a thin spiral streamer of ink which, when cells were present, showed characteristic 'breaks' at intervals equal to the cell wavelength. At low flow-rates, a broad band of ink was first formed with Ω set far below the critical point and after a few minutes Ω was raised to the desired value. Both methods were used in the region $6 < R_x < 12$, yielding the same results. Factor (*d*) results in spuriously low values of Ω_c at $R_x \sim 0$. To obviate this difficulty, we measured the time which it took for the cells to appear in our region of observation when Ω was suddenly raised to the desired value. This time was over 5 min for a large ($\sim 3\,\%$) range of Ω, but decreased rapidly beyond a certain value of Ω. By verifying visually the slow time as being due to the propagation of cells from the ink ports, we identified the point of sudden change as Ω_c.

The weakness of the cell patterns means that the determination of Ω_c still remains somewhat dependent on the judgement of the observer. At least two of the authors participated in the determination of every point presented in this paper, thus compensating somewhat for individual eccentricities of judgement. Our estimated probable error in Ω_c is $\pm \frac{1}{3}\,\%$, which agrees well with the scatter in our data (see figure 2).

(ii) *Non-axisymmetric modes.* Non-axisymmetric disturbances of two types were observed to occur (see §4.2). Since these were superimposed on the axisymmetric pattern, their onset was considerably more difficult to observe, especially when axial flow was present. Our procedure again was to establish a broad band of evenly distributed ink at low Ω, and then to bring Ω to the desired value. We estimate the uncertainty in Ω_c for these modes to be of the order of $\pm \frac{2}{3}\,\%$.

4. Results and discussion

4.1. *Axisymmetric mode*

In figure 2 we show the results obtained in the manner described above, each point representing an individual determination of T_c. The solid curve is that calculated by Krueger & DiPrima (1964) in the narrow-gap limit, and it falls slightly below our experimental points. Donnelly & Schwarz (1964) find that the exact value at $R_x = 0$ and $\eta = 0{\cdot}95$ is $T_c = 1755$. If we assume that the finite-gap effect is about the same for small finite R_x, then the theoretical curve should be raised by about 45 Taylor numbers. The errors in Ω_c and temperature lead to an expected vertical scatter of $\pm \frac{2}{3}\,\%$ in our points. In addition, the uncertainty of $\pm \frac{1}{2}\,\%$ in the absolute value of the viscosity makes the vertical position of the

curve as a whole uncertain by $\pm 1{\cdot}0\,\%$, or about 20 Taylor numbers. In view of this, the absolute agreement with theory is excellent.

Plotting the slope $\Delta T_c/\Delta R_x$ of the experimental curve against $\bar{R}_x$ (figure 3), we find a definite discontinuity at $\bar{R}_x \simeq 16$. (The slope is calculated by taking the difference in average T_c and the difference in average R_x between neighbouring groups of points, and dividing the one by the other. $\bar{R}_x$ is the mean R_x between

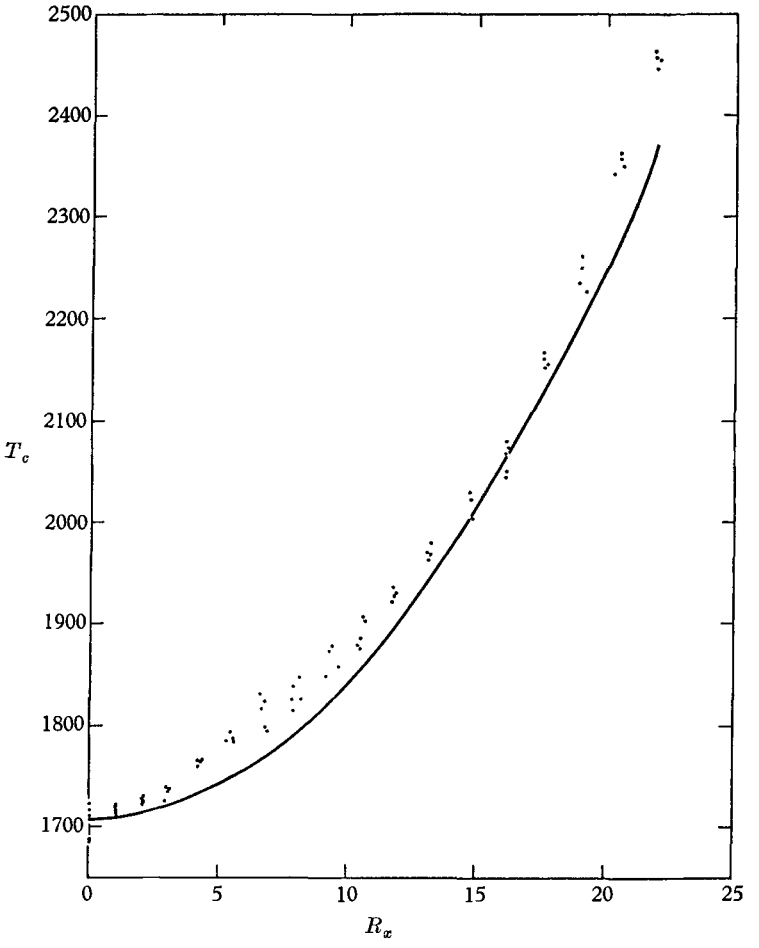

FIGURE 2. Dependence of the critical Taylor number T_c on axial Reynolds number R_x. Dots represent experimentally determined points and the full-line curve is that calculated by Krueger & DiPrima (1964).

two groups of points.) This discontinuity is in the neighbourhood of the point where Snyder found the wave-number of the cells to depart significantly from the theoretical values (Snyder 1962, figures 6 and 7). By means of photographs, we measured the angle that the cells make with the horizontal. The results (figure 4) show that near $R_x = 15$ the cell pattern becomes spiral (as suggested by Snyder) rather than toroidal. Thus, above $R_x = 15$, the theoretical curves are not strictly applicable. It is somewhat surprising that for R_x above this value the experimental points still fall very near the curve calculated on the basis of a toroidal disturbance.

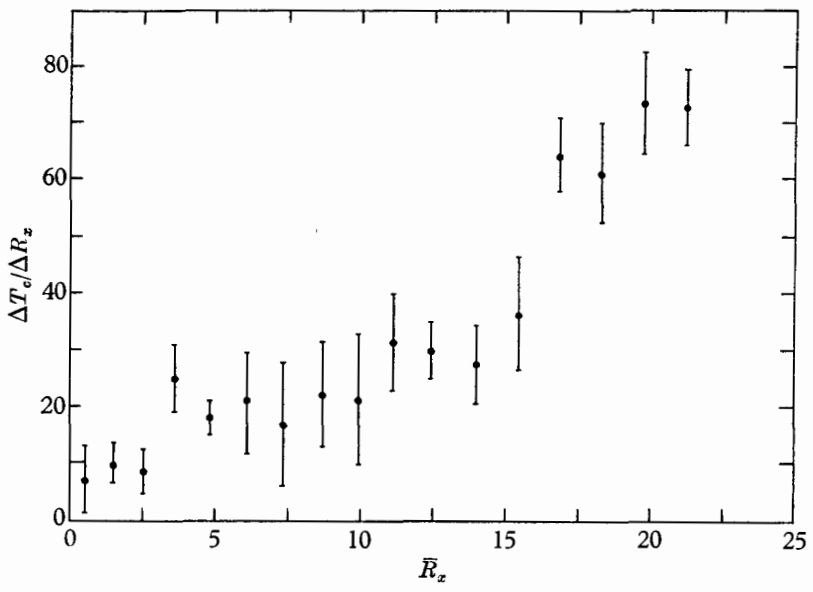

FIGURE 3. Dependence of average slope, $\Delta T_c/\Delta R_x$, of the experimental curve on $\bar{R}_x$. The break at $\bar{R}_x \simeq 16$ coincides with the value of R_x at which spiral cells are first observed.

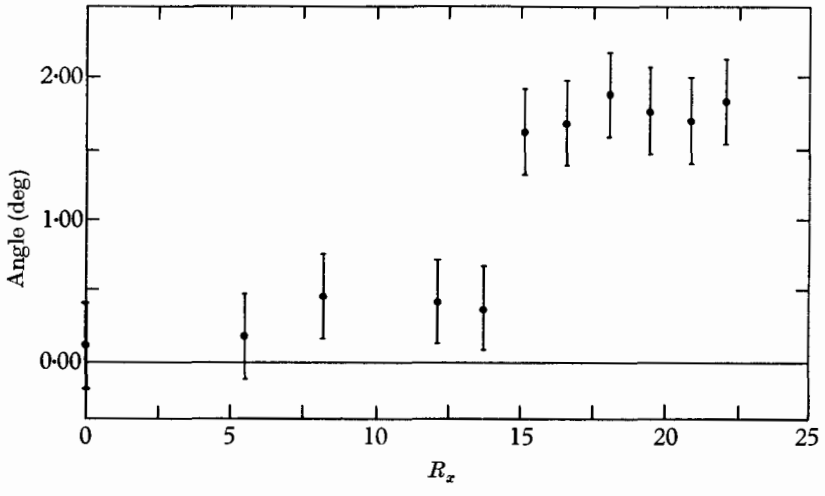

FIGURE 4. Dependence on R_x of the angle the cells make with the horizontal. The break at $R_x \simeq 15$ indicates the onset of spiral cells. Each point is the average of eight measurements.

4.2. *Non-axisymmetric modes*

The types of stable cell patterns observed are pictured in figure 5, plate 1. These photographs were all taken with $R_x = 0$, but small flow-rates did not affect the qualititative behaviour of these patterns. Figure 5(*a*), plate 1, is typical of the axisymmetric mode, the cell wavelength here being $\sim 0{\cdot}70$ cm at a Taylor number of 1780. As T is increased, the pattern changes to one of alternating

light and dark bands (figure 5(*b*)) characteristic of the weak non-axisymmetric modes. Each band varies as $\exp i(\theta - \omega t)$, switching from light to dark with a well-defined frequency, and exactly out of phase on opposite sides of the cylinder. There is no doubt that this pattern corresponds to the $m = 1$ mode postulated by DiPrima (1961). To demonstrate its existence explicitly, we show a sequence of photographs in figure 6, plate 2, taken at about 2 sec intervals. By noting the variation of intensity with time at a fixed height on the scale, the changes in phase of the pattern can easily be seen. Donnelly & Fultz (1960*a*) noticed variations of intensity with time which they ascribed to overstable oscillations. On page 1152 of their paper, they say 'The overstable oscillations appear as periodic changes in the apparent density of ink lines between the cells'. They quote a period of $\sim$ 12 sec for the oscillations, and it is probable that they were seeing the $m = 1$ mode.

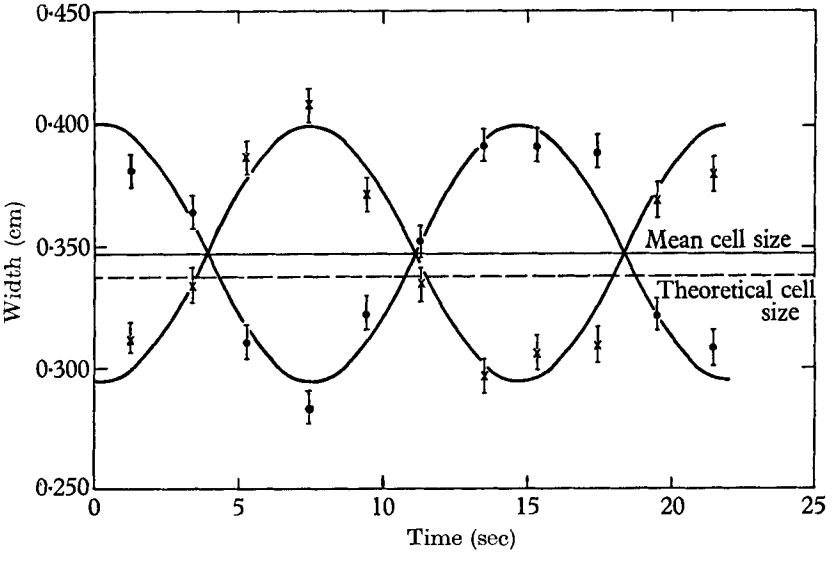

FIGURE 7. Variation of the widths of the light and dark bands observed in the strong $m = 1$ mode at a fixed azimuth. Since a complete cells includes one light and one dark band, this shows the periodic distortion of the axial cos kz dependence of the cell shape. Here, dots are averages of the widths of eight neighbouring dark bands; crosses are averages of the widths of the corresponding eight light bands.

Theoretically, we expect $\omega = 0{\cdot}513\Omega_c$ at the onset of the $m = 1$ mode. By analysing a sequence of photographs taken at $T = 1937$, we found

$$\omega = (0{\cdot}54 \pm 0{\cdot}03)\,\Omega_c,$$

the large error being due to the difficulty of deciding when the pattern had shifted through a complete cycle. The agreement is good despite the fact that we are about 7 % above the $m = 1$ critical point. Contrary to the usual theoretical assumption that the symmetric and non-symmetric modes are independent, we find that the $m = 1$ mode is always locked in on the symmetric pattern. Thus, it first appears as a subtle modification of the symmetric mode rather than as a new cell pattern superimposed with arbitrary vertical phase.

No stable modes of the type $\exp i(m\theta - \omega t)$ with $m > 1$ were observed with our narrow gap. When T is increased, the circulation in the $m = 1$ mode grows more vigorous and the axial waveform becomes distorted, perhaps because of an interaction with the axisymmetric pattern. The distortion at first takes the form of a sinusoidal variation in the widths of the bands, as shown in figure 7. Figure 5 (*c*)

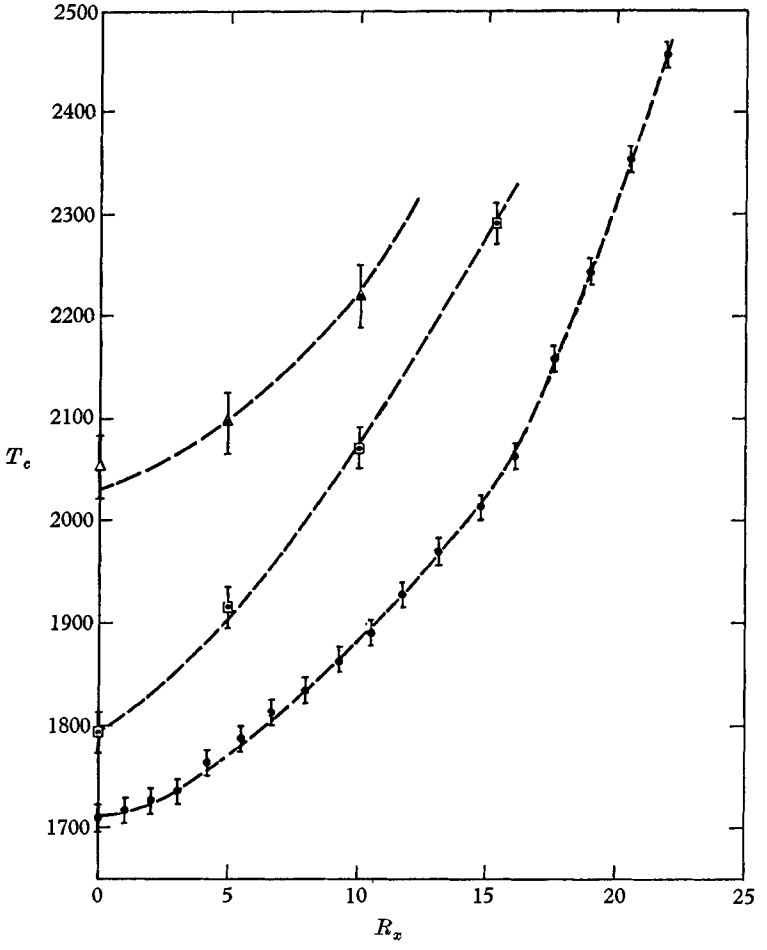

FIGURE 8. Dependence of average experimental values of T_c on R_x for the axisymmetric, the $m = 1$, and the completely non-symmetric modes. The dashed curves are fitted by eye to the points. ●, axisymmetric mode; □, $m = 1$ mode; Δ, completely non-symmetric mode.

shows the distorted cells and also demonstrates the difference in phase on opposite sides of the cylinder. As T is increased still further, the phase change becomes increasingly sudden until finally a discontinuity develops, as in figure 5 (*d*). This 'bump' sets in at a well-defined Taylor number and is stable. It does not appear to be an independent mode of instability, seeming rather to be caused by the interaction of the $m = 1$ mode with the axisymmetric mode.

In figure 8 we show the T_c versus R_x curves obtained for the axisymmetric, the $m = 1$, and the completely non-symmetric modes. They are seen to be roughly

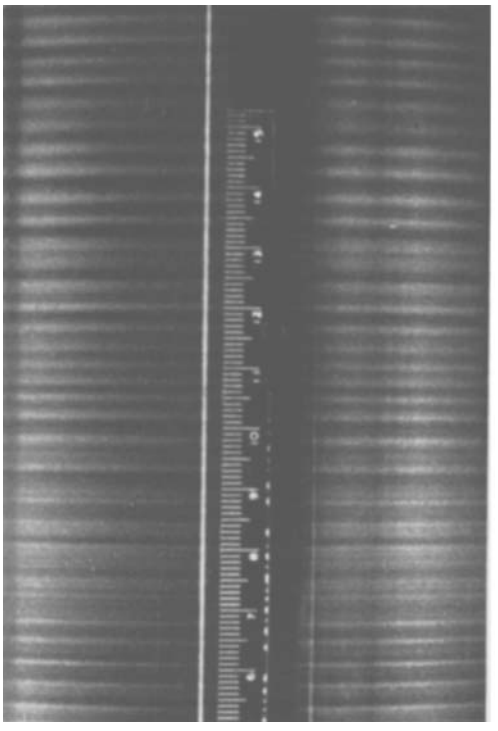

(*a*)

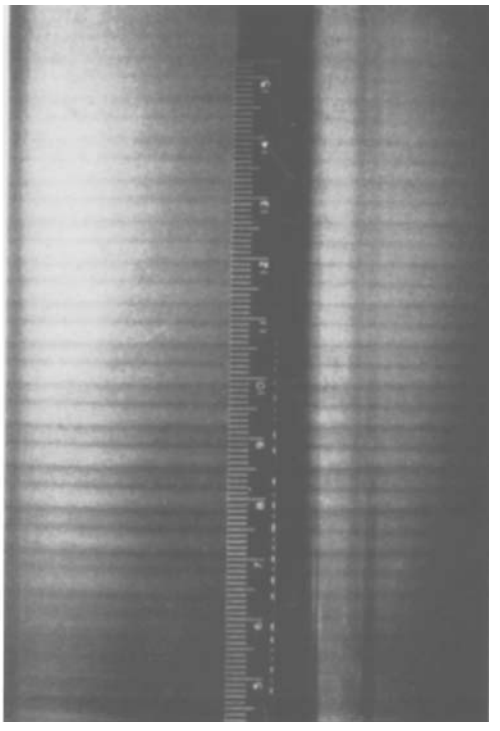

(*b*)

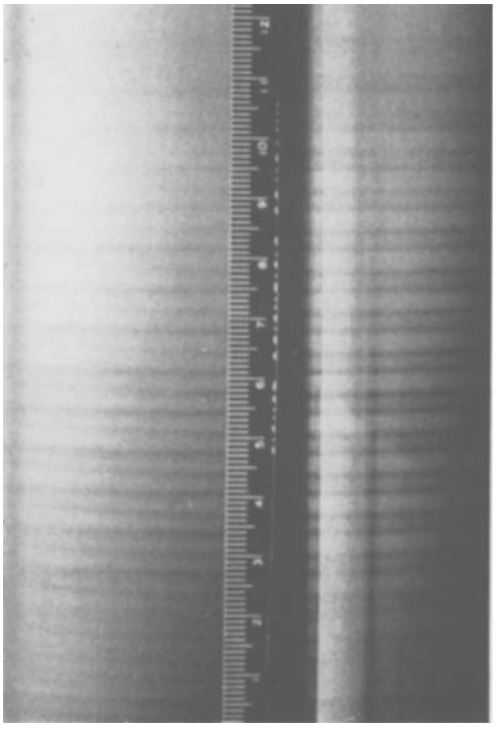

(*c*)

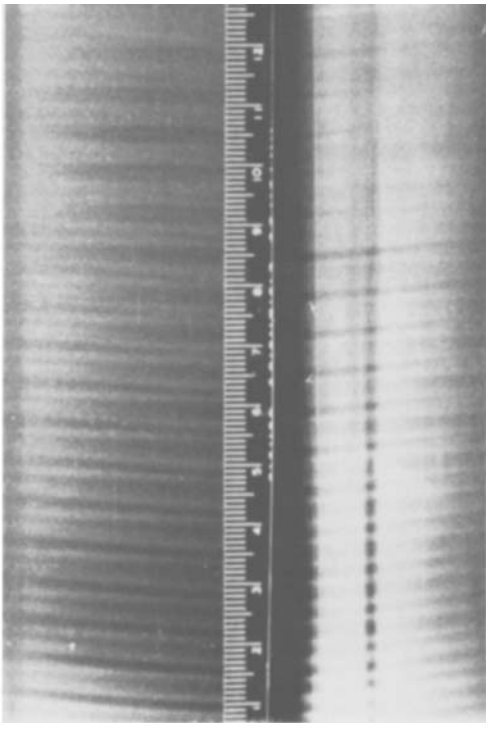

(*d*)

FIGURE 5. Typical appearance of the various modes of instability, with $R_x = 0$ in each case. (*a*) Axisymmetric mode ($T = 1780$); (*b*) weak $m = 1$ mode ($T = 1937$); (*c*) $m = 1$ mode with some distortion ($T = 2116$); (*d*) completely non-symmetric 'bump' ($T = 2348$).

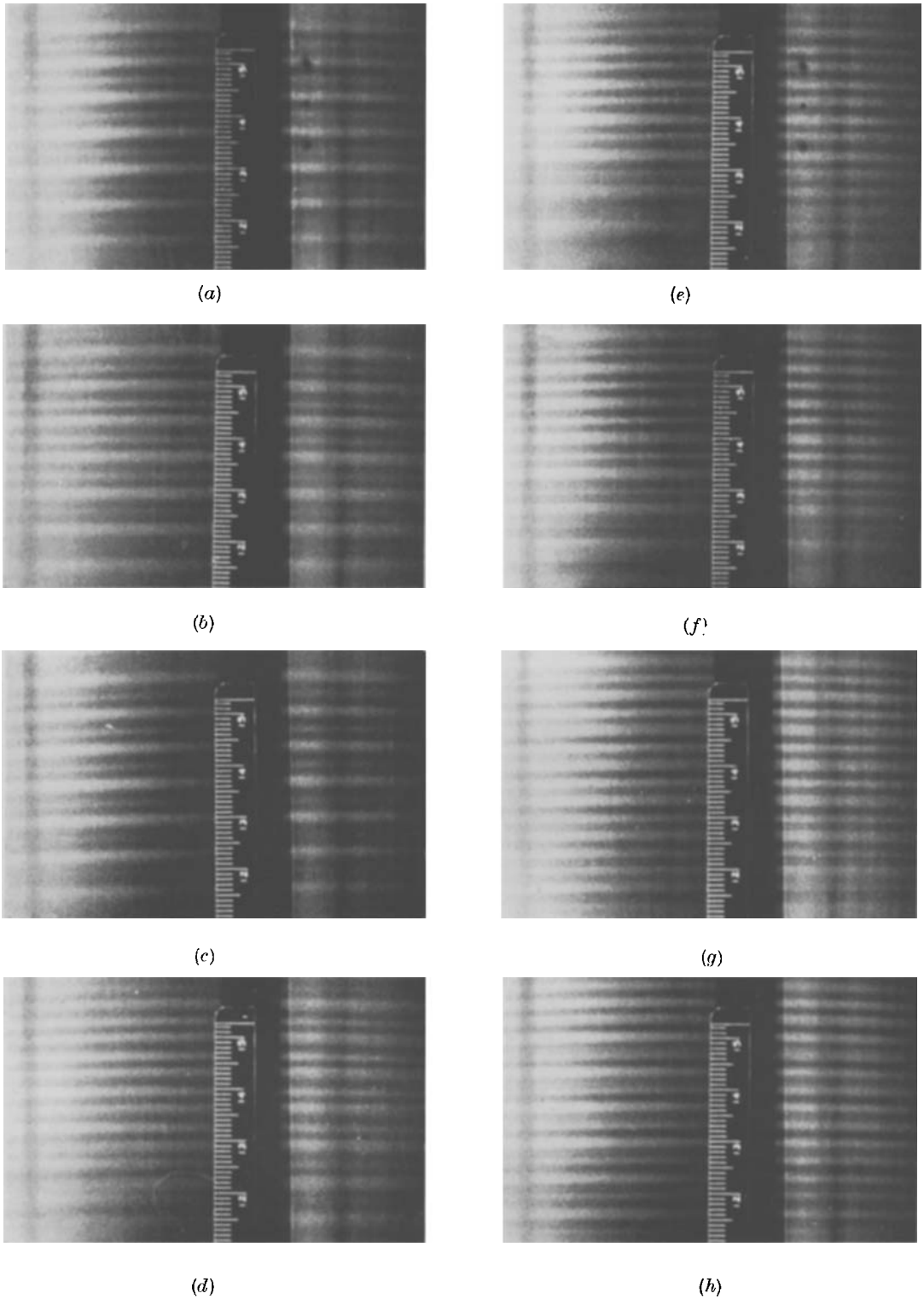

FIGURE 6. Sequence of eight photographs showing the appearance of the $m = 1$ mode over an interval of 13 sec. Note that in photographs separated by an interval of 7 sec, the positions of light and dark bands are interchanged ($R_x = 0$ and $T_c = 1916$). (*a*) $t = 0{\cdot}00$ sec, (*b*) $t = 1{\cdot}80$ sec, (*c*) $t = 3{\cdot}72$ sec, (*d*) $t = 5{\cdot}74$ sec, (*e*) $t = 7{\cdot}50$ sec, (*f*) $t = 9{\cdot}16$ sec, (*g*) $t = 11{\cdot}05$ sec, (*h*) $t = 13{\cdot}29$ sec.

SCHWARZ, SPRINGETT AND DONNELLY

parallel. The one available theoretical prediction concerning the azimuthal modes is that at $R_x = 0$, $T_c = 1763$ for the $m = 1$ mode (see Donnelly & Schwarz 1964; DiPrima 1961; Krueger, Gross & DiPrima 1964). That this is somewhat below the experimental value is perhaps due to the assumption in the theory that the $m = 1$ mode is completely independent of the axisymmetric mode.

5. Conclusions

The flow between rotating cylinders with a narrow annulus (with the outer cylinder stationary) was observed to have three distinct types of instability, each with a well-defined value of T at which they become self-sustaining: the familiar axisymmetric mode, the first azimuthal mode of the form $\exp i(\theta - \omega t)$, and a completely unsymmetric instability apparently dependent on the interaction of the $m = 1$ and axisymmetric modes. The qualitative behaviour of these patterns was not affected by small flow-rates up to $R_x = 20$.

The effect of R_x on T_c was quantitatively determined for low R_x. In the axisymmetric case, the results are in excellent agreement with the theoretical predictions of Krueger & DiPrima. The non-symmetric modes show a similar dependence on R_x, although they occur at higher Taylor numbers.

We are indebted to Prof. Dave Fultz for the use of his laboratory facilities and for a number of helpful discussions in these experiments. We are also indebted to Prof. R. C. DiPrima for discussions of his theoretical results in advance of publication. This research has been supported by the Office of Naval Research under a contract Nonr-2121(20) with the University of Chicago and by the National Science Foundation under a grant G-23068 for the Physics of Fluids. Research activities of the Institute for the Study of Metals are supported by general grants from the U.S. Atomic Energy Commission and the Advanced Research Projects Agency. During the period of this research, one of us (Russell J. Donnelly) held an Alfred P. Sloan Research Fellowship.

REFERENCES

CHANDRASEKHAR, S. 1960 *Proc. Nat. Acad. Sci. Wash.* **46**, 141.
CHANDRASEKHAR, S. 1962 *Proc. Roy. Soc.* A, **265**, 188.
DIPRIMA, R. C. 1960 *J. Fluid Mech.* **9**, 621.
DIPRIMA, R. C. 1961 *Phys. Fluids*, **4**, 751.
DONNELLY, R. J. & FULTZ, D. 1960*a* *Proc. Nat. Acad. Sci. Wash.* **46**, 1150.
DONNELLY, R. J. & FULTZ, D. 1960*b* *Proc. Roy. Soc.* A, **248**, 101.
DONNELLY, R. J. & SCHWARZ, K. W. 1964 *Proc. Roy. Soc.* A (to be published).
KRUEGER, E. R. & DIPRIMA, R. C. 1964 *J. Fluid Mech.* **19**, 528.
KRUEGER, E. R., GROSS, A. & DIPRIMA, R. C. 1964. Submitted to *J. Fluid Mech.*
SNYDER, H. A. 1962 *Proc. Roy. Soc.* A, **265**, 198.